# Diffusion Monte Carlo calculation of rate of elastic transmission of a helium vapor beam through a slab of superfluid helium

Y. Lutsyshyn[1] and J. W. Halley[2]

[1]*Departament de Física i Enginyeria Nuclear, Universitat Politècnica de Catalunya,Campus Nord B4-B5, E-08034, Barcelona, Spain*

[2]*School of Physics and Astronomy, University of Minnesota, Minneapolis, Minnesota 55455, USA*

(Received 26 October 2009; revised manuscript received 8 July 2010; published 12 January 2011)

We present the results of diffusion Monte Carlo calculations of the elastic transmission of a low-energy beam of helium atoms through a suspended slab of superfluid helium. These calculations represent a significant improvement on variational Monte Carlo methods which were previously used to study this problem. The results are consistent with the existence of a condensate-mediated transmission mechanism, which would result in very fast transmission of pulses through a slab.

DOI: 10.1103/PhysRevB.83.014504 PACS number(s): 67.25.bf, 67.25.dp

## I. INTRODUCTION

There are very few experimental confirmations[1,2] of the existence of a Bose condensate, first postulated by London,[3] in superfluid $^4$He. The most direct of such experiments are deep inelastic neutron-scattering measurements.[1,2] Several years ago[4–7] we proposed that observation of anomalous elastic helium atom transmission would also be an experimental signature of the existence of a condensate. We argued that the quantum mechanical amplitudes for absorption and re-emission of bosons (say from state $\lambda$) from a system in which there are already $n_\lambda$ bosons present are respectively enhanced by factors $\sqrt{n_\lambda + 1}$ and $\sqrt{n_\lambda}$. Because of this effect, absorption and re-emission of helium atoms are strongly enhanced. Further insight is obtained by consideration of the one-body density matrix $\rho_1(\vec{r},\vec{r}')$,[8–10]

$$\rho_1(\vec{r},\vec{r}') = \langle \Phi_N \mid \psi^\dagger(\vec{r}')\psi(\vec{r}) \mid \Phi_N \rangle, \tag{1}$$

where $\Phi_N$ is the $N$-body ground state of the system and $\psi^\dagger(\vec{r}')$ and $\psi(\vec{r})$, respectively, create a particle at $\vec{r}'$ and destroy a particle at $\vec{r}$. The condensate fraction $n_0$ is related[8] to the one-particle density matrix in the limit $|\vec{r} - \vec{r}'| \to \infty$ as $\rho_1(\vec{r},\vec{r}') \to n_0(N/V)$, where $V$ is the volume of the system. Because the one-body density matrix is the overlap between a wave function with one extra particle at $\vec{r}'$ and a wave function with one extra particle at a faraway point $\vec{r}$, one may expect that processes in which a particle is added at $\vec{r}$ and removed at $\vec{r}'$ will be observable with amplitudes essentially independent of the distance between the two points. The proposed transmission experiment would add and remove particles from the fluid in this way in order to probe the structure of the one-particle density matrix at large spatial separations. Transmission takes place through a virtual quantum-mechanical process, quantum mechanically mixing the state consisting of a free particle and the $N$-particle Bose-condensed liquid ground state and a (boosted) state consisting of $N + 1$ particles in the Bose-condensed liquid ground state. These states differ in energy by an energy of the order of the chemical potential of about 7 K, so one expects a time delay of the order of $\hbar/7$ K $\approx 10^{-12}$ s for the re-emission of the incident atom. We made previous estimates of the transmission amplitude and phase for this process, both phenomenologically[4] and variationally,[5] with results consistent with the uncertainty principle estimate. The $k$ dependence of the amplitude of the condensate mediated transmission, if observed, might provide some direct information about the structure of the condensate.

In the real system, other processes will compete with the proposed condensate-mediated process when a low-energy ($\approx$1 K) helium atom is incident on the fluid. These include both inelastic processes, such as those accompanied by the creation of one or more ripplons which do not result in transmission, as well as the elastic creation of a (real, not virtual) roton or phonon with atomic absorption followed by roton or phonon destruction together with atomic remission. We reviewed the possible inelastic processes in Ref. 11. In the present paper we only consider the elastic channel and do not obtain any estimate of the relative magnitude of elastic and inelastic channels. However, we point out that, as reviewed briefly in what follows, there are both experimental and computational indications that a substantial fraction of incident helium atoms result in elastic transmission. What we do obtain from the calculation described here is an estimate of the amplitude and phase of the transmission coefficient of condensate mediate transmission in the elastic channel. This permits estimates of the relative probability of elastic transmission and reflection as a function of incident momentum, as well as the time delay associated with elastic transmission. Within the context of studying only the elastic channel, there is also the question of the relative probability of roton- and phonon-mediated transmission and coherent, condensate-mediated transmission. In principle, the methods described here can address this question, but, as described in the Conclusion, the implementation of the method in the calculation presented here has not yet yielded a definitive answer to this last question. (The competition between quasiparticle-mediated transmission and condensate-mediated transmission has some physical similarities to the competition between recoilless emission of $\gamma$ rays and emission accompanied by phonon production in the Mössbauer effect.)

Three helium atom transmission experiments have been reported: Wyatt and co-workers[12] carried out an experiment on an array of superfluid helium tubes and reported roton-mediated atomic transmission. Incident atomic energies were up to 4.5 K above the vacuum level. Lidke and co-workers reported an experiment[13] on a film of superfluid suspended in a cesium-coated orifice and reported transmission which they attributed to phonon-mediated transmission. Neither of

 

these papers reported a prompt signal of the sort expected for condensate mediation. Of the various possible reasons for this, one is that, in both experiments, the superfluid sample is strongly coupled to its environment (a tube or an orifice) and this may make the envisioned current carrying "boost" of the superfluid in the virtual intermediate state difficult to achieve. A third experiment by Harms and Toennies[14] measured energy and momentum transfers from an essentially stationary $^4$He vapor to moving superfluid $^4$He droplets. The lowest internal excitation energy (in the reference frame of the droplet and relative to the ground state energy of the droplet) of $^4$He atoms entering the droplet was around 12 K (about 5 K relative to vacuum), which is around the "maxon" feature in the helium superfluid excitation spectrum. At such energies, inelastic multiple quasiparticle excitation dominates elastic transmission.

A correlated basis function calculation of transmission amplitudes arising from quasiparticle creation and annihilation was reported in Ref. 15. The method appears to explicitly exclude a virtual condensate mediated mechanism, but allows inelastic processes. Substantial fractions (of order 10% or more depending on wave vector) of incoming beams were predicted to be transmitted elastically in those calculations.

The variational Monte Carlo calculations which we reported earlier[5] gave a large condensate-mediated transmission amplitude consistent with earlier calculations and arguments. However, all variational calculations of that type depend on the choice of variational wave function and one could argue that the results might have arisen because the choice of variational wave function was too constrained. In that calculation, as in the one reported here, one is calculating properties of an excited scattering state, so the usual variational methods need to be modified to assure that the variational procedure does not simply take the calculation back to the ground state. In principle, this is not a problem, because the scattering boundary conditions constrain the wave function not to describe the ground state, but, for strongly interacting systems, there are no standard, generally accepted methods for carrying out such calculations. In previous work[5] we used a variational method called "minimizing the fluctuations of the local energy" by Krotscheck *et al.*[16] to estimate the transmission coefficients.

Here we describe a nonstandard application of the fixed-node approximation in diffusion Monte Carlo to fix the boundary conditions and calculate the properties of the required excited state. This is similar in spirit to the approaches of Carlson, Pandharipande, and Wiringa,[17] Alhassid and Koonin,[18] and Shumway and Ceperley[19] for three-dimensional scattering problems in small systems. However, it is important to emphasize that the method we are using is different in important details from the ones used in the cited papers. For example, we do not use the methods of Ceperley and Bernu[20] to calculate a convergent spectrum of excited states, as done in Ref. 19. Instead, we determine the phase shifts by requiring that the lowest energy consistent with a given boundary condition fixed by the phase shifts be equal to the value of the energy required for elastic transmission. [See Eq. (16), which is an implicit equation for the phase shift at wave vector $k$.] This method can only be used for the elastic channel, whereas the method of Ref. 19 also yields estimates for inelastic channels. On the other hand, as we show, we can use our method to obtain results (albeit only for the elastic channel) for substantially larger systems.

Diffusion Monte Carlo (DMC) calculations are, in principle, exact and represent an improvement on our previous variational Monte Carlo methods. For practical application, DMC calculations require a "trial function" which plays a role somewhat like the variational function in variational Monte Carlo calculations. However, DMC calculations can give final results for the wave function which are very different from the trial wave function, whereas in variational Monte Carlo calculations, the variational function fixes the form of the final calculated result. In practice, in our fixed node approach, the trial function does impose some constraints on the final DMC result, but the result will be much closer to the exact one than that resulting from a variational Monte Carlo calculation.

In the next section we describe the methods. In the third section we present results, and in the last section we provide conclusions and discussion.

## II. DIFFUSION MONTE CARLO METHOD

The DMC method for determining the properties of strongly interacting quantum systems (for which there is no convergent perturbation expansion) was was proposed by Anderson[21,22] and developed in the 1970s and 1980s with the addition of importance sampling, fixed-node, and node-release methods.[23–28]

To find the properties of the ground state of a system, DMC iterates the operator $e^{-(\mathcal{H}-E_{\rm ref})\tau}$ on an initial wave function $\Psi_I$ until contributions from all the excited states vanish, leaving only a term $e^{-(E_0-E_{\rm ref})\tau}\phi_0$, where the ground-state wave function $\phi_0$ has energy $E_0$. The resulting $\tau$ dependence can be used to determine the ground-state energy and other ground-state properties. To describe the method in more detail, let $\phi_n(X)$ be the (unknown) energy eigenstates of the system's Hamiltonian (here $X$ denotes a set of coordinates of all the particles in the system):

$$\mathcal{H}\phi_n(X) = E_n\phi_n(X).$$

Then, in principle, it is possible to expand

$$\Psi_I = \sum_n \langle\Psi_I|\phi_n\rangle\phi_n(X) = \sum_n A_n\phi_n(X), \tag{2}$$

defining $A_n$. Let a function $f(X,\tau)$ be defined as

$$\begin{aligned} f(X,\tau) &= \Psi_T(X)e^{-(\mathcal{H}-E_{\rm ref})\tau}\Psi_I(X) \\ &= \Psi_T(X)\sum_n \exp[-(E_n - E_{\rm ref})\tau]A_n\phi_n(X). \end{aligned} \tag{3}$$

$\Psi_T$ is usually taken to be real. In most cases one also takes $\Psi_I = \Psi_T$. Apart from the factor $e^{E_{\rm ref}\,\tau}$, the function $f(X,\tau)$ is $\Psi_T$ times the evolution of $\Psi_I$ in imaginary time.

If the reference energy $E_{\rm ref}$ is equal to the ground-state energy, then

$$\lim_{\tau\longrightarrow\infty} f(X,\tau) = \Psi_T(X)A_0\phi_0(X),$$

so that

$$\frac{1}{\Psi_T(X)}\lim_{\tau\longrightarrow\infty} f(X,\tau) \propto \phi_0(X), \tag{4}$$

because the exponential factors in the sum will cause all terms in Eq. (3) for which $E_n > E_0$ to vanish in the limit of large $\tau$. It is said that excited states are projected out of the initial $\Psi_I$. If $E_{\rm ref} \neq E_0$, then $f(X,\tau)$ either vanishes or diverges at large $\tau$. Therefore, if a value is found for $E_{\rm ref}$ such that $f$ neither vanishes nor diverges, then the ground-state energy $E_0 = E_{\rm ref}$ and the ground-state wave function is given by (4). (It is assumed that $\Psi_T$ has nonzero overlap with the ground state $\phi_0$ so that $A_0 \neq 0$.) In order to compute $f(X,\tau)$ one computes its time derivative with respect to $\tau$ using (3),

$$\frac{\partial}{\partial\tau} f(X,\tau) = -\Psi_T(X)\,(\mathcal{H} - E_{\rm ref})\,\frac{f(X,\tau)}{\Psi_T(X)}.$$

Using the explicit form of the kinetic energy in the Hamiltonian for a nonrelativistic collection of particles, the evolution of $f$ can be rewritten as

$$\frac{\partial f}{\partial\tau} = \sum_i \frac{\hbar^2}{2m_i}\left[\nabla_i^2 f - \nabla_i(f\nabla_i \ln|\Psi_T|^2)\right] - \left(\frac{\mathcal{H}\Psi_T}{\Psi_T} - E_{\rm ref}\right) f. \tag{5}$$

One interprets the last equation by regarding $f$ as a density function in the multidimensional ($3\times$ the number of particles) configuration space in which each "system point," is a set of coordinates for all the particles in the system. (This is only possible if $\Psi_T$ is real.) We represent this function by an ensemble of system points. The first term corresponds to diffusion, the second term (under the sum) corresponds to drift of the points representing $f$ with a velocity field $\nabla \ln|\Psi_T|^2$, and the last (branching) term represents a source or sink for system points. The value of $E_{\rm ref}$ at which the number of system points is not changing during the simulation is the ground-state energy. At this same value of $E_{\rm ref}$ the distribution of system points represents the ground-state wave function (4).

To use DMC for an excited state requires some modification. In the case of the problem at hand, we impose a constraint on the imaginary time evolution, such that the density $f$ describes a wave function consistent with elastic scattering boundary conditions which exclude the ground state. We will show that an appropriate constraint can be imposed by use of an appropriate trial function.

For the transmission problem, the boundary conditions on the many-body wave function for $N+1$ particles (of which 1 may be considered to be the incident particle and $N$ to be in the target superfluid) for the elastic scattering and transmission of a low-energy atom incident normally with energy $\epsilon_{\vec{k}} = \hbar^2k^2/2m$ on a slab containing $N$ particles are described as follows:

$$\Psi(\vec{r}_1^{\,\perp},\ldots,\vec{r}_{N+1}^{\,\perp},z_1,\ldots,z_{N+1}) \underset{z_i\to\pm\infty}{\longrightarrow} \psi_k^{\pm}(z_i)\Psi_N(\vec{r}_1,\ldots,\vec{r}_{i-1},\vec{r}_{i+1},\ldots,\vec{r}_{N+1}). \tag{6}$$

[These are $2(N+1)$ conditions.] Here

$$\psi_k^{+}(z_i) = T_k e^{ikz_i} \tag{7}$$

and

$$\psi_k^{-}(z_i) = e^{ikz_i} + R_k e^{-ikz_i}. \tag{8}$$

$\Psi_N(\vec{r}_1,\ldots,\vec{r}_{i-1},\vec{r}_{i+1},\ldots,\vec{r}_{N+1})$ is the ground state of the $N$-particle slab system with the indicated coordinates. Here we chose a system of coordinates in which the $z$ axis is perpendicular to the slab surface, that is in the transmission direction, and we label the remaining transverse coordinates as $\vec{r}^{\,\perp}$, so that individual particle's coordinates can be written as $\vec{r}_i \equiv (\vec{r}_i^{\,\perp},z_i)$ and the entire set of atomic coordinates comprising a coordinate of a system in the configuration space as $X \equiv (\{\vec{r}_i\}) \equiv (\{\vec{r}_i^{\,\perp}\},\{z_i\})$. The notation $z_i \to \pm\infty$ denotes the many-body limit,

$$z_1,\ldots,z_{N+1} \longrightarrow z_1,\ldots,z_{i-1},\pm\infty,z_{i+1},\ldots,z_{N+1}, \tag{9}$$

for any $i$ and all $\vec{r}_i^{\,\perp}$. We employ periodic boundary conditions with respect to all the transverse directions, so that the wave function is periodic with respect to all the transverse components $\vec{r}_i^{\,\perp}$. Note that not more than one atomic coordinate may be allowed to approach infinity at a time, as long as the energy of the incoming particle is insufficient to knock out more than one atom from the slab, and therefore the wave function must tend to zero for configuration-space coordinates with more than one $z_i$ far from the slab. Similarly, a state in which none of the $z_i$'s is allowed to extend infinitely from the slab cannot describe an *elastic* transmission process. (As discussed in the Introduction, we are restricting attention to wave functions describing elastic processes.) In the elastic scattering problem the energy is constrained to be $\hbar^2k^2/2m + E_N$, where $E_N$ is the ground-state energy of the target superfluid slab. In the method we use, which is not the same as that used in Ref. 19, for a given $k$ we fix the phase of the incoming and out going wave, use DMC to calculate the resulting energy, and then vary the phase until the resulting energy is the correct one for the elastic channel as given earlier. [Also, see Eq. (16).] In that way we determine the phase for that $k$. However, to implement the method we needed to use real-valued wave functions as scattering states. We describe the resulting even and odd state boundary conditions next.

To apply the DMC method to this problem one cannot use precisely the boundary conditions used in Ref. 5 and described in the preceding paragraph because the wave functions involved are not real. We can obtain information about the wave function satisfying these boundary conditions by reformulating the problem in terms of scattering states which are eigenstates (even and odd) of the operation of reflection about the center of the slab, extending a method used by Poulson and Molmer for the analogous problem in the case of a weakly coupled Bose gas.[29] In empty space at fixed $k$, single-particle eigenstates with the required even and odd character are simply $\cos(kz)$ and $\sin(kz)$. In the scattering problem the corresponding single-particle phase-shifted states are

$$\begin{aligned}\psi_k^e &= \cos[kz + \delta_e(k)\,\mathrm{sgn}z] = \cos[k|z| + \delta_e(k)],\\ \psi_k^o &= \sin[kz + \delta_o(k)\,\mathrm{sgn}z] = \mathrm{sgn}(z)\sin[k|z| + \delta_o(k)],\end{aligned} \tag{10}$$

which are easily seen to have even and odd parity and correspond to appropriately phase-shifted versions of $\cos(kz)$ and $\sin(kz)$ with phase shifts $\delta_e(k)$ and $\delta_o(k)$. [These phase-shifted functions have discontinuities at the origin but the discontinuities are irrelevant to our discussion because the functions Eq. (10) are only used to establish boundary conditions at $z \to \pm\infty$.] It is straightforward to show that

$$\psi_k(z) = e^{i\delta_e}\psi_k^e(z) + i\,e^{i\delta_o}\psi_k^o(z) \tag{11}$$

gives

$$\psi_k(z) = \begin{cases} e^{ikz} + R_k e^{-ikz} & \text{for} \quad z < 0, \\ T_k e^{ikz} & \text{for} \quad z > 0, \end{cases} \tag{12}$$

with coefficients given by

$$\begin{aligned} R_k &= \tfrac{1}{2}(e^{2i\delta_e} - e^{2i\delta_o}), \\ T_k &= \tfrac{1}{2}(e^{2i\delta_e} + e^{2i\delta_o}). \end{aligned} \tag{13}$$

Therefore, if we solve the many-body Schrödinger problem with the boundary conditions

$$\begin{aligned} &\Psi^{e,o}(\vec{r}_1^{\perp}, \ldots, \vec{r}_{N+1}^{\perp}, z_1, \ldots, z_{N+1}) \\ &\quad \underset{z_i \to \pm\infty}{\longrightarrow} \psi_k^{e,o}(z_i) \Psi_N(\vec{r}_1, \ldots, \vec{r}_{i-1}, \vec{r}_{i+1}, \ldots, \vec{r}_{N+1}), \end{aligned} \tag{14}$$

with an appropriately symmetrized wave function and the energy $E = \hbar^2 k^2/2m + E_N$, then the resulting even and odd phase shifts can be used to determine the transmission and reflection coefficients for the elastic scattering and transmission problem using (13). The advantage of proceeding in this way is that $\Psi^{e,o}$ are real, permitting an adaptation of the DMC.

To enforce the boundary conditions (14) on the wave functions during the DMC evolution, we use a trial function of form

$$\begin{aligned} &\Psi_{\mathrm{T}}^{e,o}(r_1^{\perp}, \ldots, r_{N+1}^{\perp}, z_1, \ldots, z_{N+1}) \\ &\quad = \sum_{i=1}^{N+1} \psi_k^{e,o}(z_i) \Psi_{N+1;i}(r_1, \ldots, r_{N+1}). \end{aligned} \tag{15}$$

Here $\Psi_{N+1;i}(\vec{r}_1, \ldots, \vec{r}_{N+1})$ is a nodeless function, localized in the neighborhood of the slab and specified in what follows. These trial functions will satisfy the boundary conditions as long as

$$\Psi_{N+1;i}(\vec{r}_1, \ldots, \vec{r}_{N+1}) \to \Psi_N(\vec{r}_1, \ldots, \vec{r}_{i-1}, \vec{r}_{i+1}, \ldots, \vec{r}_{N+1})$$

in the limits $z_i \to \pm\infty$ described earlier. The nodes of $\Psi_{\mathrm{T}}^{e,o}$ are then fixed by the factors $\psi_k^{e,o}(z_i)$. These nodes, in turn, fix the boundary conditions because, in the limit of large (positive or negative) $z_i$, the wave function of an isolated particle far from the slab with nodes fixed by $\psi_k^{e,o}(z_i)$ will necessarily be a sine or cosine function with the phase of $\psi_k^{e,o}(z_i)$. Because, in the fixed node approximation which we use, the system points of the DMC evolution cannot cross the nodal configuration space hypersurfaces of the trial function, the boundary conditions will be preserved during the DMC evolution with these trial functions.

In outline, our calculational procedure is then as follows: For a given value of $k$ we solve the implicit equation for the phase shifts given in (16) by choosing a series of trial values of the phase shifts $\delta_e(k)$ and $\delta_o(k)$ and performing a DMC calculation for each choice with the corresponding trial function. (We do two DMC calculations, one even and one odd, for each candidate choice of the trial phase shifts, for each value of $k$.) Evaluating the resulting energies $E[\delta_{e,o}(k)]$ from the DMC calculations for a series of phase shifts, we then determine the correct phase shifts by solving the implicit relations

$$E[\delta_{e,o}(k)] = \hbar^2 k^2/2m + E_N. \tag{16}$$

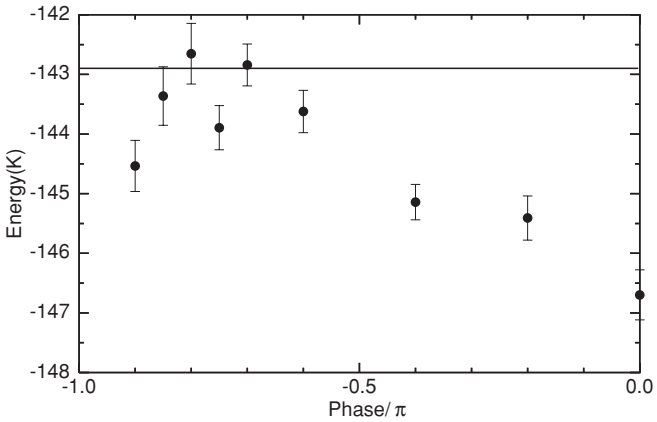


FIG. 1. An example of a calculation of an even phase shift. $k = 0.65$ Å$^{-1}$. The plot shows the DMC determined energy of the scattering state for a series of possible phase shifts. Each energy value is the result of a separate simulation using a different phase shift in the trial function given by Eq. (15). The correct even phase shift for this $k$ is that for which the calculated energy is equal to the known energy at this $k$ [the right-hand side of Eq. (16)] which is $-142.9$ K for this $k$, as indicated by the horizontal line. The error bars on the DMC points show the statistical error in the energy. The figure illustrates how the implicit Eq. (16) for the even phase shift is solved. For this value of $k$ the right-hand side of Eq. (16) is $-142.9$ K and the phase $\delta_e(k = 0.65$ Å$^{-1})$ is thus determined to lie between $-0.65\pi$ and $-0.85\pi$. Such "phase scans" were repeated for each wave vector for both symmetries.

(For each $k$ there is one relation for the even phase and a second relation for the odd phase). This imposes the correct requirement on the energy as described earlier. The process of solving Eq. (16) is illustrated in Figs. 1 and 2 . The DMC results for the various trial phase shifts are the data points and the value of the right-hand side of Eq. (16) is shown as a horizontal line. A correct phase shift for the wave vector is then estimated from the data by estimating the point at which a curve through the data points passes through or touches the horizontal line. If there were more than one channel for elastic transmission and reflection, this process could give, in principle, multiple solutions for the phase shifts. If we succeed in finding a scattering state by this procedure, then, if the DMC is fully converged, it will be an eigenstate at the excited-state energy and will therefore be orthogonal to all lower energy states, as required. States describing inelastic scattering channels will have different boundary conditions.

For a full description of the procedure, it remains to specify the functions $\Psi_{N+1;i}(r_1, \ldots, r_{N+1})$ which we so far said needed to be nodeless, localized near the slab, and obeying the limit $\Psi_{N+1;i}(r_1, \ldots, r_{N+1}) \to \Psi_N(r_1, \ldots, r_{i-1}, r_{i+1}, \ldots, r_{N+1})$. We have chosen the form

$$\begin{aligned} &\Psi_{N+1;i}(r_1, \ldots, r_{N+1}) \\ &\quad = [1 - f(z_i^*)] \prod_{j \neq i} f(z_j^*) \Psi_{\mathrm{Jastrow}}^{N+1}(r_1, \ldots, r_{N+1}), \end{aligned} \tag{17}$$

in which $z_i^* = z_i - \sum_{s=1}^{N+1} z_s/(N+1)$ and

$$f(z_i) = \left(\frac{1}{e^{(z_i - a)/b} + 1}\right)\left(\frac{1}{e^{(-z_i - a)/b} + 1}\right), \tag{18}$$

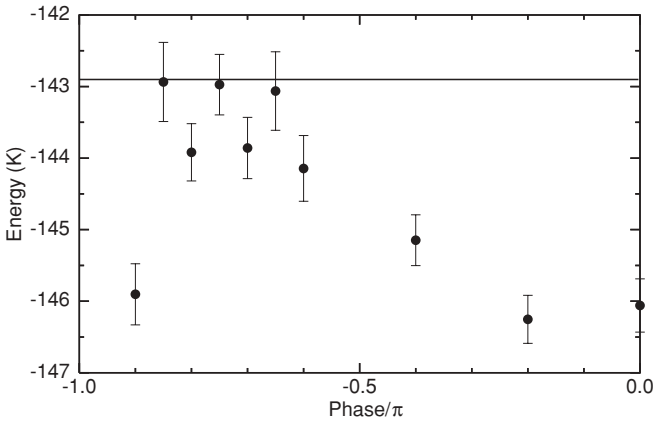


FIG. 2. An example of a calculation of an odd phase shift for the same $k$ value $k = 0.65$ Å$^{-1}$ used to obtain the results shown in Fig. 1 , but using the scattering state trial function with odd symmetry. Phases $\delta_o$ and $\delta_e$ are determined only to within a multiple of $\pi$, as can be seen by examining Eq. (15).

where $a$ and $b$ are parameters roughly describing the width and position of the edges of the slab. Notice that the function is chosen to be a function of particle position relative to the center of mass of the slab. $\Psi^{N+1}_{\text{Jastrow}}(r_1, \ldots, r_{N+1})$ is the Jastrow function for the ground-state bulk helium problem with $N + 1$ particles in the McMillan form:

$$\Psi^{N+1}_{\text{Jastrow}}(r_1, \ldots, r_{N+1}) = \prod_{i,j=1\, i\neq j}^{N+1} \exp[-(c/r_{ij})^5]. \qquad (19)$$

The resulting trial functions are essentially the same as the first term in the variational function used in our previous variational Monte Carlo calculations[5] (after resummation to form the appropriate incident, scattered and transmitted plane waves as described earlier.) The Fermi-function like forms are known to describe helium surfaces well.[25,30] The main defect in this trial function is that it does not locally conserve current in the center of the slab. In Ref. 5 we used a second term in the variational wave function to correct this defect. In the calculations presented here we depend on the DMC evolution toward a correct wave function to assure local current conservation. We discuss this further in the final section.

## III. CALCULATIONS AND RESULTS

In this section we present results of 32-particle transmission simulations. In fixed node approximation, the boundary conditions are fixed by the trial function specified in Eqs. (15), (17), (18), and (19). The interaction between helium atoms is assumed to be of two-body Lennard-Jones type with de Boer-Michels coefficients[31]: $V(r_{ij}) = 4\epsilon[(r_0/r_{ij})^{12} - (r_0/r_{ij})^6]$, with $\epsilon = 10.22$ K and $r_0 = 2.556$ Å. More accurate two-body potentials[32–35] could be used within the method without serious complications but were deemed unnecessary at this stage of the work. We used $c = 2.235$ Å . Box transverse dimensions were $6.15 \times 6.15$ Å and film parameters were set at $a = 19.7$ Å (half thickness) and $b = 0.49$ Å (corresponding to 10%–90% surface layer width of 1.8 Å). We used an imaginary time step of $10^{-4}$ K$^{-1}$ for $5 \times 10^5$ steps, resulting in a total projection time of 50 K$^{-1}$. Each simulation involved an average of 500 system points, but no more than 1000. We used a second-order integration method as proposed by S. Chin.[36] This method, classified as DMC 2a in Ref. 36, has been tested on helium[37] and on systems with nodal wave functions.[38] The method provided good convergence for our problem. The system was allowed to equilibrate from the initial conditions for the first one-fifth of the run. Equilibration was monitored by recording energy and density histograms and the system was found to be well equilibrated within the allotted period.

It is unusual to calculate an excited state with as many as 32 particles using this type of method. It was possible[39] by our use of the method described earlier, which is different from others cited in the Introduction. The price we paid for this advantage is that we could only study the elastic transmission channel. However, even with 32 particles the results suffered from finite size effects.

The energy that corresponds to the correct scattering phase as described previously is given by the right-hand side of Eq. (16). It includes the energy of an $N$-particle film (while the entire transmission system involves $N + 1$ particles). In the case of a 32-particle transmission, this calls for a simulation of the ground state of a 31-particle film. Such a simulation may be biased because of suboptimal filling of the simulation volume. In the vicinity of $N = 32$, however, we find nearly linear variation of the ground-state film energy with the number of particles. The level of nonlinearity determines the possible filling effects, which we estimate to be smaller than 1 K. This is comparable to our typical statistical uncertainty of about half a degree. Assuming linearity with particle number we have estimated the ground-state energy of a 31-particle film as (31/32) times our calculated ground-state energy of a 32-particle film and used that value in Eq. (16). Other reasonable estimates for $E_N$ give the same values for the scattering phases within our statistical uncertainties.

Phases were extracted from each such calculation as described earlier (see the final paragraph of the preceding section) and a range of admissible ranges for the amplitude and phase of the transmission coefficients as a function of $k$ were calculated with the help of Eqs. (13) and (16) with results shown in Figs. 3 and 4. [Note that in Figs. 1 and 2, the

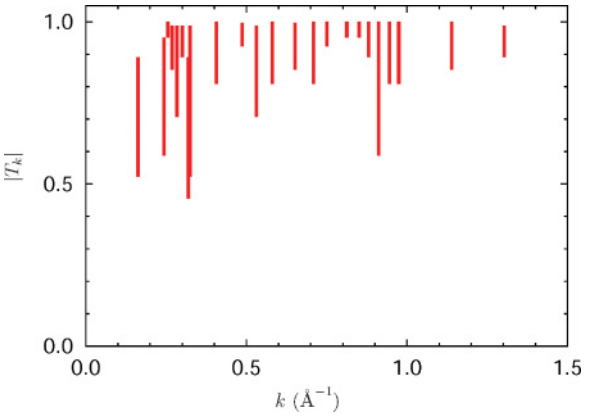


FIG. 3. (Color online) Absolute value of the transmission coefficient vs the impact particle's wave vector during elastic scattering events. Bars indicate uncertainty.

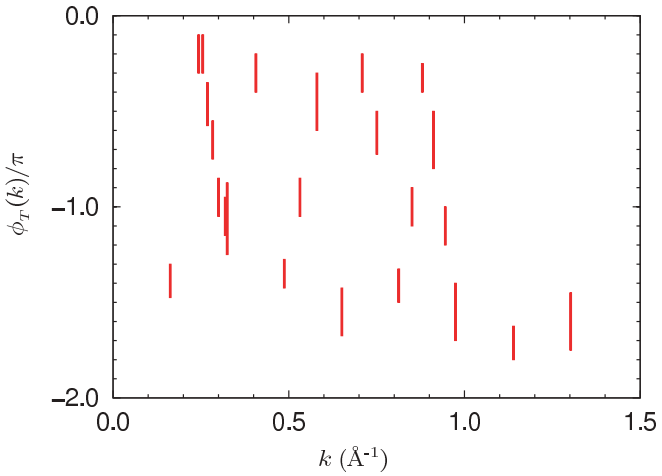


FIG. 4. (Color online) The phase of the transmission coefficient determined from the even and odd phase shifts using Eq. (13). The phases have been shifted to lie in the interval 0 to $-2\pi$. The bars indicate the uncertainty. The phase as a function of $k$ changes rapidly, forming a repeating stripe pattern. Same data is shown in Fig. 5.

only physically significant phase shifts are those which solve Eq. (16). These figures illustrate the method used for solving the implicit Eq. (16) for the correct phases for this $k$.] The magnitude of the transmission coefficient turned out to be very close to unity, implying nearly complete elastic transparency at most incident wave vectors. There is some structure and diminution of the calculated $|T_k|$ at low wave vectors. This may be an artifact of the fact that the wavelength of the incoming particle becomes commensurate with the size of the slab at these $k$'s.

Calculated results for the phase of the transmission coefficient are shown in Fig. 4. In Fig. 5 the calculated phases have been shifted by factors of $2\pi$ to produce a phase which varies

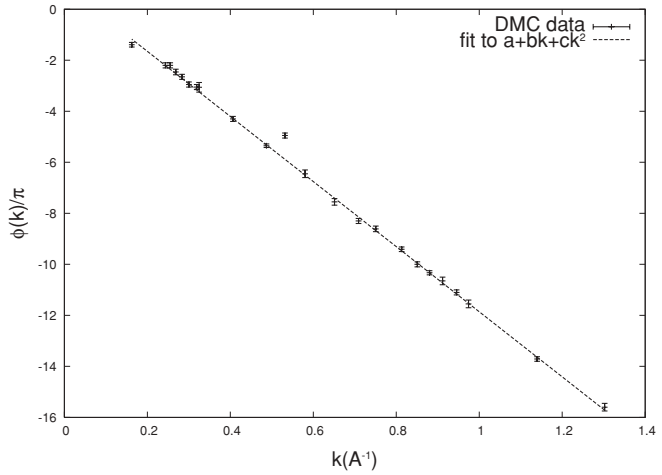


FIG. 5. The phase of the transmission coefficient, shown here with the phases shifted by multiples of $2\pi$ to form a continuous function, using the same data (including the same error bars) which were used to plot Fig. 4. The line is a polynomial fit to all the data except for the outlier point at $k = 0.53$ Å$^{-1}$, as described in the text.

smoothly with $k$. The shifted phases are seen to very nearly fall on a straight line with negative slope.

## IV. DISCUSSION AND CONCLUSIONS

The phase of the transmission coefficient can be used to extract some information about transmission times which we can use to infer something about probable transmission mechanisms. If we form a wave packet using the emitted waves, it is of form

$$\psi(z,t) = \int \frac{dk}{(2\pi)} g(k) \exp[i(\vec{k}\cdot\vec{r} - (\hbar k^2/2m)t + \phi(k)],$$

where $\phi(k)$ is the phase of $T(k)$. (We assume that the wave packet is of infinite extent in the direction parallel to the slab surface.) We expand the phase to second order in $k$,

$$\phi(k) = \phi_0 + k d\phi/dk|_0 + (1/2)k^2 d^2\phi/dk^2|_0,$$

which clearly works over the range for which we measured $\phi(k)$ (Fig. 5). The origin of the expansion can be taken to be $k = 0$, as is done here. Now we assume that $g(k)$ varies more slowly about its maximum than the rate of variation of the phase with $k$ near the maximum in $g(k)$. To evaluate this assumption we note that $g(k)$ is a product of $|T(k)|$ and a factor arising from the shape of the incoming incident wave packet. The factor $|T(k)|$ clearly varies much more slowly than the phase over the range of $k$ for which it was calculated (Fig. 3). The variation of the factor associated with the incoming wave-packet shape depends on the experimental preparation of the incoming beam. Normally, from thermal sources, one obtains a Gaussian wave packet in the moving frame with a spatial width of the order of the thermal wavelength associated with the temperature in the moving frame. In the pulses used in some recent experiments[40] the temperatures in the moving frame varied between 0.01 and 1 K, corresponding to thermal wavelengths from about 10 to 100 Å. In the low end of this range the packet shape is varying more slowly with wave vector than the phase in the present calculation, for which $d\phi/dk \approx -40$ Å though not in the high end of the range, corresponding to internal pulse temperatures of 10 mK. However, under experimental conditions $d\phi/dk$ will be of the order of the slab width, which is likely to be considerably larger than 40 Å and in such cases the assumption of a slowly varying envelope in $k$ space should be valid. With that assumption we obtain by evaluation of the integral by steepest descent that the spatial peak of the emerging wave packet will occur at the position at which the derivative of the phase in the preceding equation is zero, namely,

$$z + d\phi/dk|_0 + k_0 d^2\phi/dk^2|_0 - (\hbar k_0/m)t = 0,$$

where $k_0$ is the position of the peak, in $k$, of the incident wave packet. For comparison with a freely propagating wave packet with a peak in $k$ at the same wave vector value $k_0$ in the absence of the slab of superfluid helium, we take the origin of $z$ far to the left of the left (incident) edge of the slab and consider $z$ far to the right of the right edge of the slab. Denoting $v_{k_0} = \hbar k_0/m$

the group velocity of the freely propagating wave packet, we have

$$t = (z + d\phi/dk|_0)/v_{k_0} + (m/\hbar)\, d^2\phi/dk^2|_0$$

for the arrival time $t$ of the spatial peak of the transmitted wave packet at $z$, whereas the spatial peak of the freely propagating wave packet leaving the origin at the same time would arrive at the same value of $z$ at time $t'$ given by

$$t' = z/v_{k_0}.$$

In close analogy to the definition of scattering length in low-energy scattering from central potentials,[41,42] we define the scattering width of the slab as $L = -d\phi/dk|_0$. Then the difference between the arrival time $t$ in the presence of the slab and the arrival time $t'$ in the absence of the slab is

$$t - t' = -L/v_{k_0} + (m/\hbar)\, d^2\phi/dk^2|_0.$$

Thus, the predicted propagation time is reduced by the time required for a free wave packet to pass through a region having a width equal to the slab scattering width plus a contribution from the curvature term. If the curvature term were zero, we could interpret this to mean that the time for propagation through the region of width equal to the scattering width was zero. Hence, the curvature term may be interpreted as the "time delay" experienced by a particle upon transmission through the slab.

We find that the data in Fig. 5 can be very accurately fit to a quadratic form in $k$ if the point at 0.53 Å$^{-1}$ is omitted. We find a slope of $-40.1$ Å corresponding to a scattering width of 40.1 Å and a curvature corresponding to $(m/\hbar)\, d^2\phi/dk^2|_{k_0} = 1.4 \times 10^{-15} \pm 4.9 \times 10^{-13}$ s (goodness of fit 0.496, reduced $\chi^2$ of 0.9). The fit is much worse if the point at 0.53 Å$^{-1}$ is included and we believe that this point may represent some effects of roton-mediated transmission, though we do not have sufficient data to confirm this. The value of the scattering width obtained is very close (equal within the uncertainties) to the slab width which we obtain by other, less precisely defined, procedures. The value found for the curvature term is consistent within the uncertainty principle estimates cited earlier and with the results of Ref. 5 (and also with zero "time delay").

During some of the simulations we observed very large error bars or obtained energy values which were clearly not consistent with a differentiable dependence of the energy on the phase shifts in (16). In these cases configurations in which one particle was far from the slab were dominant. When the fixed trial phase was far from the correct physical one, these states contributed negligibly to energy averages in long calculations. In cases in which the fixed phase was close to the correct one, the contribution of such states was harder to eliminate by extended calculation. This is understood and in fact expected. In such cases, the energy at the fixed phase, involving an ensemble of configurations with the scattered particle near as well as far from the slab, has an energy quite close to the energy of a configuration in which one particle is far from the slab. Therefore, in an imaginary time simulation, though the state with a particle far from the slab will be eventually eliminated in favor of the correct one, the difference between the decay rate of that state and the correct one will be small and will get smaller as the fixed phase gets closer to the correct one. This is exactly the qualitative behavior which we observe in the calculations.

In conclusion, we have developed a version of the DMC method for study of the problem of transmission of an incident low-energy beam of helium atoms in vapor phase through a suspended slab of superfluid helium. To fix the scattering boundary conditions and avoid decay of the imaginary time trajectories of the DMC method to the ground state, we fix nodes of the trial wave function outside the slab. By doing successive calculations with varying positions of these nodes, we obtain the energy as a function of the scattering wave function phase shift. We then obtain the physical phase shift by numerically solving the equation which requires the energy to be the physical energy of the ground state of the slab plus the kinetic energy of the incident particle when it is far from the slab. The procedure is carried out for both even and odd scattering states and the results are used to compute the scattering amplitude and to estimate the time delay for the transmission event. This appears to be the first DMC calculation on such a scattering problem.

From 32-particle simulations, we find very large transmission coefficients (near 1 in amplitude) and very short transmission times, consistent within the accuracy of the calculation with our earlier estimates (a fraction of a picosecond). These results are consistent with previous suggestions of a condensate-mediated mechanism for transmission, which, however, has not yet been observed experimentally.

There may be some indications in the results of the competitive, quasiparticle-mediated transmission mode, but these require further study, and it may require a different trial function to easily access the part of the Hilbert space describing quasiparticle mediation using DMC.

As discussed earlier, the trial function used here does not locally conserve current, and it is very advisable to repeat these calculations including a term, used earlier in variational Monte Carlo calculations on the same problem, which allows better local current conservation in the trial function. This would check the assumption, made in the present work, that local current conservation is adequately restored by the DMC drift-diffusion processes.

Finally, there is evidence of finite size effects in the present calculations and it would be desirable to repeat them with a larger system. However, our earlier VMC calculations,[5] which gave results very similar to the ones reported here, were done for two slab thicknesses and larger numbers of particles, giving us some confidence that the results obtained from the DMC simulations on 32 particles reported here will not be qualitatively different from those which would be obtained in larger systems.

## ACKNOWLEDGMENTS

This work was supported the Minnesota Supercomputing Institute. Y.L. did some of this work while supported by a fellowship from the School of Physics and Astronomy at the University of Minnesota. David Ceperley is thanked for some helpful discussions.

[1]P. C. Hohenberg and P. M. Platzmann, Phys. Rev. **152**, 198 (1966).
[2]P. E. Sokol and W. M. Snow, in *Excitations in Two Dimensional and Three Dimensional Quantum Fluids*, edited by A. G. F. Wyatt and H. J. Lauter (Plenum Press, New York, 1991), p. 47.
[3]F. London, Nature (London) **141**, 643 (1938).
[4]J. W. Halley, C. E. Campbell, C. F. Giese, and K. Goetz, Phys. Rev. Lett **71**, 2429 (1993).
[5]A. K. Setty, J. W. Halley, and C. E. Campbell, Phys. Rev. Lett. **79**, 3930 (1997).
[6]J. W. Halley, Physica B **197**, 175 (1994).
[7]J. W. Halley, J. Low Temp. Phys. **93**, 893 (1993).
[8]C. N. Yang, Rev. Mod. Phys. **34**, 694 (1962).
[9]O. Penrose, Philos. Mag. **42**, 1373 (1951).
[10]O. Penrose and L. Onsager, Phys. Rev. **104**, 576 (1956).
[11]A. Wynveen, K. A. Lidke, Y. Lutsyshyn, and J. W. Halley, Phys. Rev. B **75**, 054506 (2007).
[12]C. D. H. Williams and A. F. G. Wyatt, Phys. Rev. Lett. **91**, 085301 (2003).
[13]K. A. Lidke, A. Wynveen, N. Baisch, C. Koay, C. F. Giese, and J. W. Halley, J. Low Temp. Phys. **140**, 429 (2005).
[14]J. Harms and J. P. Toennies, Phys. Rev. Lett. **83**, 344 (1999).
[15]C. E. Campbell, E. Krotscheck, and M. Saarela, Phys. Rev. Lett. **80**, 2169 (1998).
[16]E. Krotscheck, G. X. Qian, and W. Kohn, Phys. Rev. B **31**, 4245 (1985).
[17]J. Carlson, V. R. Pandharipande and R. B. Wiringa, Nucl. Phys. A **424**, 47 (1984); see also K. M. Nollett, S. C. Pieper, R. B. Wiringa, J. Carlson, and G. M. Hale, Phys. Rev. Lett. **99**, 022502 (2007).
[18]Y. Alhassid and S. E. Koonin, Ann. Phys. **155**, 108 (1984).
[19]J. Shumway and D. M. Ceperley, Phys. Rev. B **63**, 165209 (2001).
[20]D. M. Ceperley and B. Bernu, J. Chem. Phys. **89**, 6316 (1988).
[21]J. B. Anderson, J. Chem. Phys. **63**, 1499 (1975).
[22]J. B. Anderson, J. Chem. Phys. **65**, 4121 (1976).
[23]J. B. Anderson, J. Chem. Phys. **73**, 3897 (1980).
[24]F. Mentch and J. B. Anderson, J. Chem. Phys. **74**, 6307 (1981).
[25]K. S. Liu, M. H. Kalos, and G. V. Chester, Phys. Rev. B **12**, 1715 (1975).
[26]D. M. Ceperley and B. J. Alder, Phys. Rev. Lett. **45**, 566 (1980).
[27]P. J. Reynolds, D. M. Ceperley, B. J. Alder, and W. A. Lester, J. Chem. Phys. **77**, 5593 (1982).
[28]J. W. Moskowitz, K. E. Schmidt, M. A. Lee, and M. H. Kalos, J. Chem. Phys. **77**, 349 (1982).
[29]U. V. Poulsen and K. Molmer, Phys. Rev. A **67**, 013610 (2003).
[30]J. M. Marin, J. Boronat, and J. Casulleras, Phys. Rev. B **71**, 144518 (2005).
[31]J. De Boer and A. Michels, Physica **6**, 97 (1939).
[32]R. A. Aziz, V. P. S. Nain, J. S. Carley, W. L. Taylor, and G. T. McConville, J. Chem. Phys. **70**, 4330 (1979).
[33]M. H. Kalos, M. A. Lee, P. A. Whitlock, and G. V. Chester, Phys. Rev. B **24**, 115 (1981).
[34]R. A. Aziz, F. R. W. McCourt, and C. C. K. Wong, Mol. Phys. **61**, 1487 (1987).
[35]R. A. Aziz, A. R. Janzen, and M. R. Moldover, Phys. Rev. Lett. **74**, 1586 (1995).
[36]S. A. Chin, Phys. Rev. A **42**, 6991 (1990).
[37]J. Boronat and J. Casulleras, Phys. Rev. B **49**, 8920 (1994).
[38]A. Sarsa, J. Boronat, and J. Casulleras, J. Chem. Phys. **116**, 5956 (2002).
[39]However, the required computation time was significant. Each energy-value point presented in the graphs in this section would take one and a half days of single-core time on a modern PC. Total wall time for 32-particle simulation results presented in Figs. 3 and 4 is almost two years.
[40]A. Wynveen, K. A. Lidke, M. C. Williams, C. F. Giese, and J. W. Halley, Phys. Rev. E **67**, 026311 (2003).
[41]L. D. Landau and E. M. Lifschitz, *Quantum Mechanics, Nonrelativistic Theory* translated by J. B. Sykes and J. S. Bell (Addison-Wesley, Reading, MA, 1965), p. 501.
[42]A. S. Davydov, *Quantum Mechanics*, translated by I. V. Schensted (NEO Press, Ann Arbor, MI, 1966), p. 395.